Convective Boiling Heat Transfer Characteristics of R410A in Microchannels

Rin Yun
Korea University

Jae Hyeok Heo
Korea University

Yong Chan Kim
Korea University

Jin Taek Chung
Korea University

CONVECTIVE BOILING HEAT TRANSFER CHARACTERISTICS OF R410A IN MICROCHANNELS

Rin Yun, Jae Hyeok Heo, Yongchan Kim[+], Jin Taek Chung

Department of Mechanical Engineering, Korea University
Anam-Dong, Sungbuk-Ku, Seoul, 136-701, Korea
[+]Phone: (82-2) 3290-3366, Fax: (82-2) 921-5439, E-mail: yongckim@korea.ac.kr

ABSTRACT

Convective boiling heat transfer coefficient and two-phase pressure drop of R410A are investigated in rectangular microchannels whose hydraulic diameters are 1.36 and 1.44 mm. The tests are conducted with a variation of mass flux from 200 to 400 kg/m^{2}s, heat flux from 10 to 30 kW/m^2, while maintaining saturation temperatures at 0, 5 and 10°C. A direct heating method is used to provide heat flux into the fluids. The boiling heat transfer coefficients of R410A in microchannels are much higher than existing data for single tubes at similar test conditions, and the effects of test conditions on the heat transfer coefficients are relatively small. The pressure drop of R410A in microchannels shows very similar trends with those in large diameter tubes. However, it yields a larger Chisholm parameter in two-phase multiplier.

1. INTRODUCTION

In recent years, a microchannel heat exchanger has been considered as an alternative to replace the existing finned tube heat exchangers in air-conditioning systems due to its compactness and excellent heat transfer performance. As noted, R410A has been widely studied as a potential alternative refrigerant because of its favorable thermodynamic properties of heat transfer and friendships with environments. Especially, R410A is appropriate for microchannel heat exchangers due to its higher working pressure and lower pressure drop characteristics, which can solve the mal-distribution problems of microchannel heat exchangers. Although there have been extensive studies related to the performance of microchannel heat exchangers with R410A, the investigations on two-phase heat transfer coefficient and pressure drop inside microchannels are very limited.

Ebisu and Torikoshi (1998) studied boiling and condensation heat transfer characteristics of R410A, R407C and R22 with a 6.4 mm inner diameter tube. R410A showed approximately 20 % and 50% higher boiling heat transfer coefficients than those of R22 and R407C, respectively. Chang et al. (2000) reported two-phase frictional pressure drops of R410A in a 5 mm tube. They proposed the modified Friedel correlation, which extended the capability of the Friedel correlation to the small diameter range. Choi et al. (2002) presented boiling heat transfer coefficients of R410A in 1.5 and 3.0 mm diameter tubes. The effects of tube diameter were clearly observed in the heat transfer coefficient. Yan and Lin (1998) investigated the characteristics of evaporation heat transfer and pressure drop for R134a flowing in 28 horizontal small tubes, each having an inner diameter of 2.0 mm. The effects of saturation temperature on the heat transfer coefficients were significant. Tran et al. (1995) measured two-phase pressure drop with three refrigerants (R134a, R12, and R113) in two small tubes with inner diameters of 2.46 and 2.92 mm and a rectangular channel (4.06 × 1.7 mm). A correlation for two-phase pressure drop of flow boiling in small channels was developed, and their data were predicted within ± 20%.

In this study, boiling heat transfer coefficients and pressure drops of R410A in microchannels are measured at various test conditions. Experimental data are compared with the existing data and prediction correlations. A correlation for the heat transfer coefficients in microchannels is proposed by considering heat transfer mechanisms in small diameter tubes. In addition, the two-phase heat transfer characteristics of R410A are compared with those of CO_2 under the same operating conditions.

2. EXPERIMENT

Fig. 1 shows a schematic of the experimental setup. The test loop consists of a magnetic gear pump, a mass flow meter, a preheater, a test section, a control tank, and a condenser. The magnetic gear pump circulates the fluid and the preheater adjusts inlet vapor quality of the test section. To measure pressures and differential pressures at the inlet and outlet of the test section, absolute pressure transducers and differential pressure transducers are installed, respectively. The accuracy of the differential pressure transducer is ±0.25 % of full scale. The mass flow rate is measured using a Coriolis effect flow meter with an uncertainty of ±0.2 % of reading. Wall temperatures of the test section and fluid temperatures are measured by T-type thermocouples with a calibrated accuracy of ±0.1°C. Applying a direct current heating method provides heat flux to the test section. The test section is insulated using rubber foam with a thermal conductivity of 0.04 W/mK to minimize heat loss to the ambient. The heat loss is estimated by comparing electric heat input with actual heat transfer rate to the fluid in terms of bulk temperature difference and mass flow rate in single-phase flow. The heat loss is within 5 % of the electric heat input, and it is taken into account in the experiments and analysis of the test data.

Test tubes have rectangular channels as shown in Fig. 2. Headers are connected to the inlet and outlet of the test section to provide stable and even distribution of the fluid. Table 1 shows the specifications of microchannels tested in this study. The experiments for the microchannels are conducted with a variation of mass flux, heat flux, and saturation temperature. Mass flux is varied from 100 to 400 kg/m^{2}s, heat flux is altered from 5 to 20 kW/m^2, and saturation temperatures are maintained at 0, 5, and 10 °C.

The local heat transfer coefficient, α, inside the microchannel is determined from the measured heat flux, Q, the fluid temperature, T_r, and the calculated inside wall temperature, T_w. The inside wall temperature, T_w, is calculated from the measured outside wall temperatures using both the equation of steady state heat conduction through the tube and heat generation within the tube wall.

$$\alpha = Q/(T_w - T_r) \quad (1)$$

Due to the difficulties in installing pressure-measuring taps on the test section without changing hole shape and making disturbance to the flow, the total pressure drop is measured at the headers that are located at the inlet and out of the test section, respectively. The net pressure drop in a microchannel is determined by subtracting contraction and expansion pressure losses and recovery at the headers from the measured total pressure drop. Eqs. (3) and (4) show a correlation for calculation of contraction losses (Coleman and Krause, 2004).

$$\Delta P_{meas} = \Delta P_{con} + \Delta P_{exp} + \Delta P_{frict} \quad (2)$$

$$\Delta P_{con} = (G^2{}_{vc}/2\rho_{tp})[(1-\sigma^2 C^2{}_c)-2C_c(1-C_c)] \quad (3)$$

$$C_c = 1- (1 - \sigma)/(2.08(1-\sigma) + 0.5371) \quad (4)$$

Table 1. Dimensions of the test tubes

Channels	Outside width (mm)	Outside height (mm)	Inside width (mm)	Inside height (mm)	Thickness A (mm)	Thickness B (mm)	Perimeter (mm)	Hydraulic diameter (mm)
7-hole	16	1.8	1.79	1.2	0.35	0.5	41.86	1.44
8-hole	16	1.8	1.57	1.2	0.35	0.5	44.32	1.36

3. RESULTS AND DISCUSSION

3.1 Heat Transfer Characteristics of R410A in Microchannels

Fig. 3 shows the heat transfer coefficients of R410A and R134a in microchannels and single tubes at various test conditions. The heat transfer coefficients of R410A in single tubes, whose diameters are from 6.4 to 1.5 mm, range from 4000 to 8000 kW/m^{2}K at various test conditions. However, the heat transfer coefficients for microchannels measured in this study show averagely 2 times larger than those for single tubes reported in the literature even though they have similar hydraulic diameters. In addition, the heat transfer coefficients of R410A in microchannels significantly increase with vapor quality as compared with those in single tubes. The R134a data in microchannels are presented to provide reference values in the comparison of the R410A data.

Fig. 4 compares the heat transfer coefficients of R410A with those of CO_2 in a microchannel with a hydraulic diameter of 1.44 mm. When heat flux increases from 10 to 15 kW/m^2 at a mass flux of 300 kg/m^{2}s and a saturation temperature of 5^{o}C, the heat transfer coefficient of R410A increases by 47 %. However, as heat flux varies from 15 to 20 kW/m^2, the variations of the heat transfer coefficients become negligible. The effects of saturation temperature and mass fluxe on the heat transfer coefficients of R410A are relatively small, while those for CO_2 are more significant.

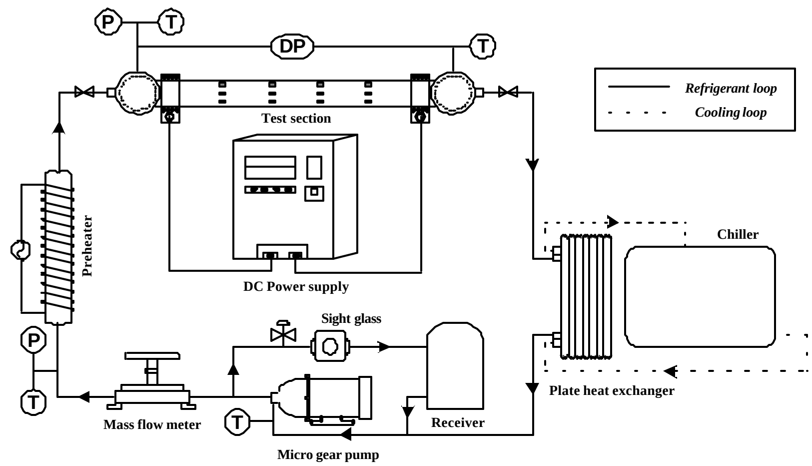

Figure 1 Schematic of experimental setup.

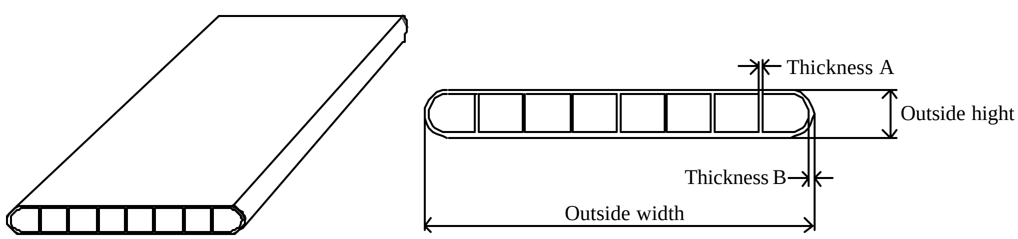

Figure 2 Details of test tube.

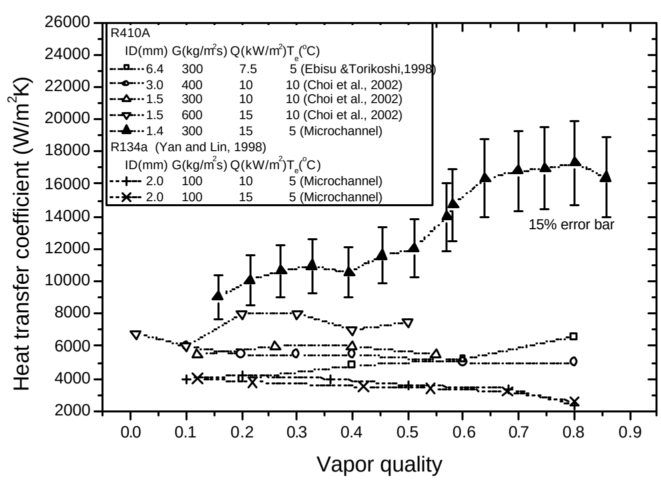

Figure 3 Comparison of the present data with existing data.

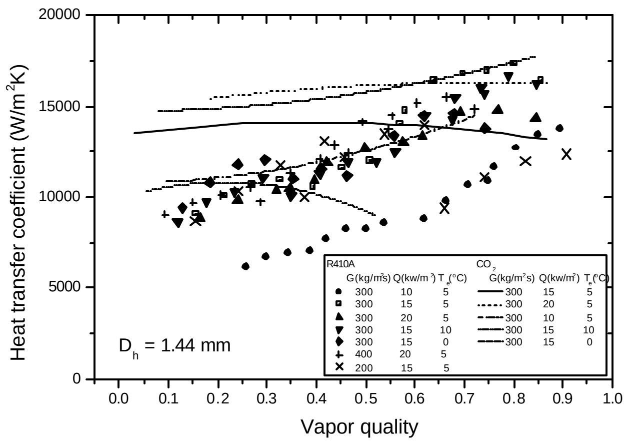

Figure 4 Heat transfer coefficients of R410A and CO_2.

Fig. 5 shows the effects of hydraulic diameter on heat transfer coefficients. As given in Table 1, the hydraulic diameters of the microchannels of 7-hole and 8-hole are 1.44 and 1.36 mm, respectively. The heat transfer coefficients of the 8-hole microchannel are averagely 25% higher than those of the 7-hole microchannel. This may be due to an increase of perimeter, which contributes on effective distribution of the heat load to each channel. In addition, the variations of the heat transfer coefficients with vapor quality in the 8-hole microchannel are smaller than those in the 7-hole microchannel. This trend indicates that nucleate boiling is much more dominate in a smaller hydraulic diameter. The active nucleate boiling and thinner liquid film at the channel wall with a decrease of tube diameter make partial dryout of the liquid film, and the heat transfer coefficients start to drop at vapor quality of 0.6 in the 8-hole microchannel. The effects of mass flux and heat flux on the heat transfer coefficients are relatively small in the tested microchannels.

Table 2 shows the existing correlations particularly developed or used for convective boiling heat transfer coefficients in small diameter tubes. *Bo* was used as an important parameter in the correlations of Lazarek and Blank (1982), and Tran et al. (1995) because the nucleate boiling was considered as the dominant two-phase heat transfer mechanism in small diameter tubes. The Cooper correlation (1984) and the Gorenflo correlation (1993) were developed to predict nucleate boiling heat transfer coefficients. Fig. 6 compares non-dimensionalized data with the predictions using the Cooper correlation (1984). α_l is calculated by the Dittus-Boelter equation. Although the Cooper correlation (1984) shows large deviations from the present data, the trends of the predictions are consistent with the measured data. Therefore, the modified Cooper correlation is suggested by multiplying 3 to the original Cooper correlation. As given in Eq. (5), a boiling heat transfer correlation is also developed by introducing the parameters proposed by Lazarek and Black (1982), and Tran et al. (1995). Fig. 7 compares the present data with the modified Cooper correlation and the present correlation. The mean deviations of the modified Cooper correlation and the present correlation are 20% and 18%, respectively. Generally, large slugs occupy most flow area in small diameter tubes at low mass flux, and the heat transfer coefficients are significantly varied by flow velocity. Therefore, it is essential to consider Reynolds number along with heat flux in the correlation.

$$\alpha = 13687\,(Bo \times We_l)^{0.1993} Re_l^{-0.1626} \tag{5}$$

Table 2. Correlations used for prediction of heat transfer coefficients in small diameter tubes

Reference	Correlation
Gorenflo (1993)	$\alpha = \alpha_o F_{PF} (q/q_o)^{nf} (R_p/R_{po})^{0.133}$
Cooper (1984)	$\alpha = 55 p_r^{0.12} (-\log_{10} p_r)^{-0.55} M^{-0.5} q^{0.67}$
Lazarek and Black (1982)	$Nu = 30 Re^{0.857} Bo^{0.714}$
Tran et al. (1995)	$\alpha = 840 (Bo^2 We_f)^{0.3} (\rho_l/\rho_g)^{-0.4}$

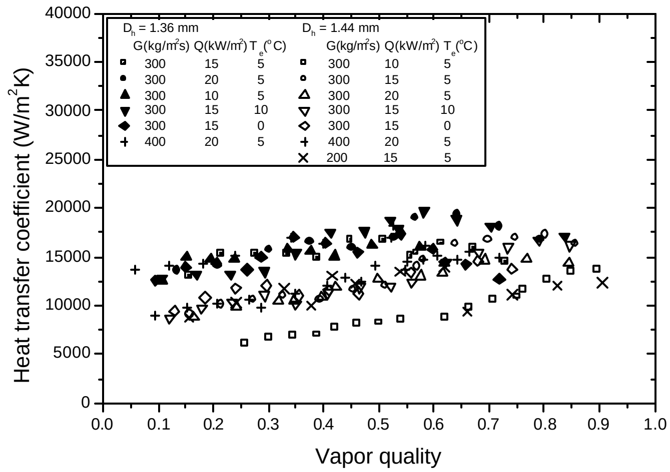

Figure 5 Effects of hydraulic diameter on heat transfer coefficients.

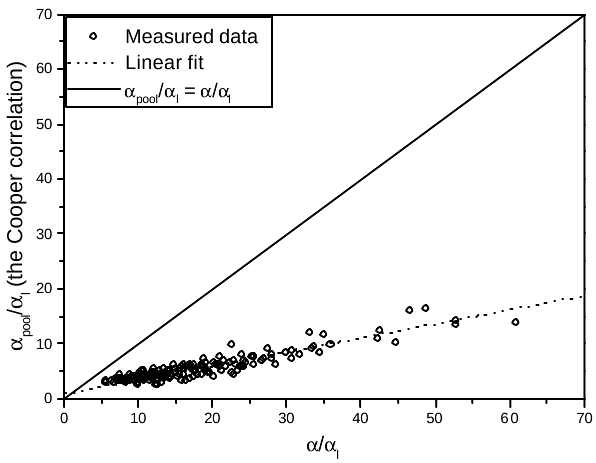

Figure 6 Comparison of the present data with the Cooper correlation (1984).

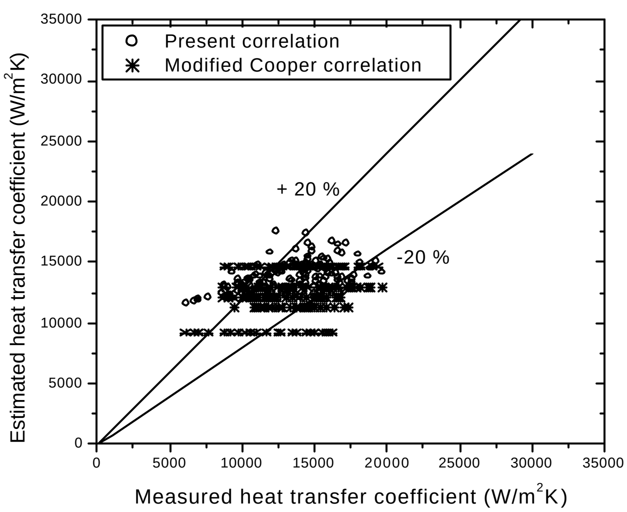

Figure 7 Comparison of the experimental data with the present correlation.

3.2 Pressure Drop Characteristics of R410A in Microchannels

Fig. 8 shows the pressure drops of R410A in a microchannel with a hydraulic diameter of 1.44 mm and a tube with an inner diameter of 5 mm (Chang et al., 2000). The pressure drops of R410A in the microchannel follow general trends observed in large diameter tubes. As the mass flux increases at a given saturation temperature, the pressure drop becomes higher. The pressure drop decreases with an increase of saturation temperature that affects viscosity and density ratio of R410A. The microchannel shows larger pressure drop than the single tube at the same mass flux and saturation temperature because of a larger perimeter of the microchannel.

Fig. 9 shows the frictional pressure drops of R410A and CO_2 in terms of two-phase multiplier (Eq. (6)) and Lockhart and Martinelli parameter (Eq. (7)). Generally, two-phase frictional pressure drops of large diameter tubes are well predicted by Eq. (6). The Chisholm parameter C in Eq. (6) varies from 5 to 21 according to flow conditions. The R410A data in the single tube with an inner diameter of 5 mm can be satisfactory correlated by varying C. In addition, the pressure drops of CO_2 obtained from this study can be well predicted by using C=21. However, the two-phase multipliers of R410A in the microchannels are much greater than those calculated by using C=21. The averaged C for R410A in the microchannels is 35. For a single tube, the Chisholm parameter C decreases with a drop of tube diameter due to a reduction of two-phase effects in small diameter tubes. The trends of pressure drop in a microchannel are quite different from those in a single tube due to an irregularity of two-phase flow entering into the channel.

$$\phi^2_{lo} = 1 + C/X_{tt} + 1/X_{tt}^2 \tag{6}$$
$$X_{tt} = (\rho_v/\rho_l)^{0.5}(\mu_l/\mu_v)^{0.125}((1-x/x)^{0.875} \tag{7}$$

Fig. 10 shows the comparison of the present data with predicted ϕ_{lo} using the Yun and Kim correlation (2003). The Yun and Kim correlation (2003) yields relatively good agreement with the R410A data in the microchannel with a hydraulic diameter of 1.44 mm, but it under-predicts the pressure drops of CO_2 and R410A in the microchannel with a hydraulic diameter of 1.36 mm. Mal-distribution to each port of a microchannel makes flow conditions very complex, which may increase ϕ_{lo}. It is also found that the increasing rate of the pressure drops for R410A and CO_2 is very similar when the microchannel diameter varies from 1.44 to 1.36 mm.

4. CONCLUSIONS

Heat transfer characteristics of R410A and CO_2 are measured in microchannels. The boiling heat transfer coefficients of R410A in microchannels are much higher than those in large or small diameter single tubes at similar test conditions. The effects of mass flux, saturation temperature, and heat flux on the heat transfer coefficients of R410A are relatively small as compared with those of CO_2. Among the existing correlations, the Cooper correlation developed for nucleate boiling shows close trends with the present data. The pressure drops of R410A in microchannels yield a large Chisholm parameter C of 35.

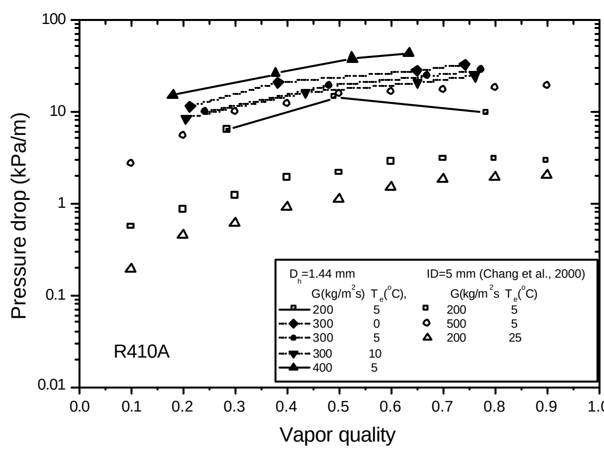

Figure 8 Effects of test conditions on two-phase pressure drop.

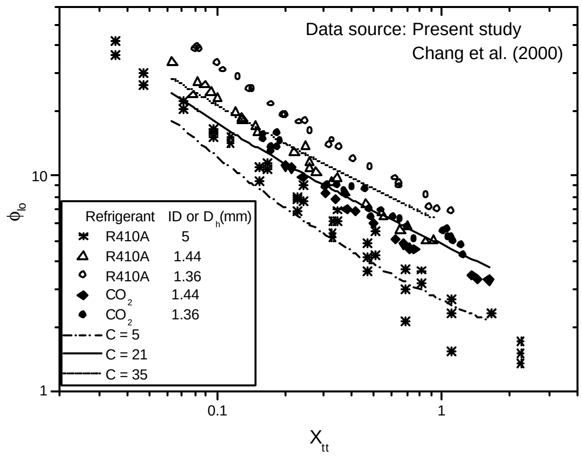

Figure 9 Two-phase multiplier vs. Martinelli parameter for the experimental data.

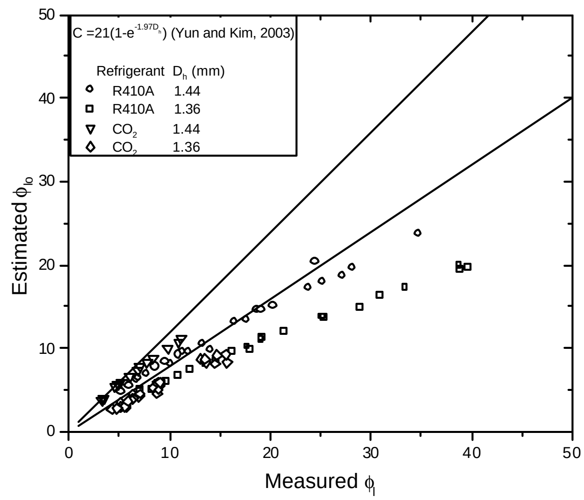

Figure 10 Comparison of the data with the predictions using the Yun and Kim correlation (2003).

NOMENCLATURE

Bo	Boiling number	
C	Chisholm parameter	
C_c	Coefficient of contraction	
D_h	Hydraulic diameter	(mm)
G	Mass flux	(kg/m^2s)
ID	Inner diameter	(mm)
Q	Heat flux	(kW/m^2)
Re_l	Reynolds number	$(G(1-x)/\mu)$
T	Temperature	(K)
We_l	Weber number based on liquid	
x	Vapor quality	
X_{tt}	Lockhart and Martinelli parameter	
α	Heat transfer coefficient	(kW/m^2K)
μ	Dynamic viscosity coefficient	(Ns/m^2)

ρ	Density	(kg/m^3)
σ	Contraction ratio	
ϕ^2_{lo}	Two-phase frictional multiplier	

Subscripts

e	Evaporation
l	Liquid
pool	Pool boiling
tp	Two-phase
v	Vapor
vc	Vena contracta

REFERENCES

Chang, Y.J., Chiang, S.K., Chung, T.W., Wang, C.C., 2000, Two-Phase Frictional Characteristics of R-410A and Air-Water in a 5 mm Smooth Tube, *ASHRAE Transactions*, vol. 109, part 1.

Cooper, M.G., 1984, Heat Flow Rates in Saturated Nucleate Pool Boiling – a Wide Ranging Examination Using Reduced Properties, in: Irvine, F. Thomas (Eds.), *Advances in Heat Transfer*, Academic Press, Orlando: p.157 – 239.

Coleman, J.W., Krause, P.E., 2004, Two-phase Pressure Losses of R134a in Microchannel Tube Headers with Large Free Flow Area Ratios, *Experimental Thermal and Fluid Science*, vol. 28: p. 123 – 130.

Choi, K.I., Pamitran, A.S., Oh, J.T., 2002, Effect on Boiling Heat Transfer of Horizontal Micro-Channel Diameter for R410A, *Proc. 2002 Winter Annual Conference*, The Society of Air-Conditioning and Refrigerating Engineers of Korea : p. 283 – 288.

Ebisu, T., Torikoshi, K., 1998, Heat Transfer Characteristics and Correlations for R-410A Flowing Inside a Horizontal Smooth Tube, *ASHRAE transactions*, vol. 104, part 2.

Gorenflo, D., 1993, Pool boiling, in: *VDI Gesellschaft Verfahrenstechnic und Chemieingenieurwesen* (Ed.), English translation of VDI, Düsseldorf: p. Ha 4 – Ha 18.

Lazarek, G.M., Black, S.H., 1982, Evaporative Heat Transfer, Pressure Drop and Critical Heat Flux in a Small Vertical Tube with R-113, *Int. J. Heat Mass Transfer*, vol. 25: p.945 – 960.

Tran, T.N., Wambsganss, M.W., France, D.M., 1995, Boiling Heat Transfer with Three Fluids in Small Circular and Rectangular Channels, *ANL-95/9*, Illinois.

Yan, Y.Y., Lin, T.F., 1998, Evaporation Heat Transfer and Pressure Drop of Refrigerant R-134a in a Small Pipe, *Int. J. Heat Mass Transfer*, vol. 41: p. 4183 – 4194.

Yun, R., Kim, Y.C., 2003, Two-Phase Pressure Drop of CO_2 in Mini Tubes and Microchannels, *First International Conference on Microchannels and Minichannels*: p.507 - 511.

ACKNOWLEDGEMENT

This work was jointly supported by the Korea Science and Engineering Foundation (Grant No. R01-2002-000-00481-0), the Korea Ministry of Commerce, Industry and Energy.